West Antarctic Surface Climate Changes Since the Mid-20th Century Driven by Anthropogenic Forcing

West Antarctic surface climate changes since the mid-20th century driven by anthropogenic forcing

Quentin Dalaiden[1], Andrew P. Schurer[2], Megan C. Kirchmeier-Young[3], Hugues Goosse[1]and Gabriele C. Hegerl[2]

[1]Université catholique de Louvain (UCLouvain), Earth and Life Institute (ELI), Louvain-la-Neuve, Belgium

[2]School of Geosciences, University of Edinburgh, United Kingdom

[3]Climate Research Division, Environment and Climate Change Canada, Toronto, ON M3H 5T4, Canada

Key Points:

- Surface climate changes since the 1950s in West Antarctica are out of the range of internal variability
- The increase in greenhouse gas emissions and stratospheric ozone depletion are responsible for these changes
- The future changes over the 21st century will depend on both the greenhouse gas emissions and the ozone layer recovery

Corresponding author: Quentin Dalaiden, quentin.dalaiden@uclouvain.be

Abstract

Although the West Antarctic surface climate has experienced large changes over the past decades with widespread surface warming, an overall increase in snow accumulation and a deepening of the Amundsen Sea Low, the exact role of human activities in these changes has not yet been fully investigated, which limits confidence in future projections. Here, we perform a detection and attribution analysis using instrumental and proxy-based reconstructions, and two large climate model simulation ensembles to quantify the forced response in these observed changes. We show that surface climate changes since the 1950s were driven by anthropogenic forcing, in particular the greenhouse gas forcing and stratospheric ozone depletion. Therefore, our results indicate that the 21st century changes will depend on both the greenhouse gas emissions and the ozone layer recovery.

Plain Language Summary

Since the second half of the 20th century, West Antarctica has experienced large climate changes, such as widespread warming, increased snow accumulation and a deepening of a low-pressure system located off the West Antarctic coasts. The observed climate changes in West Antarctica are influenced by both the internal (related to the chaotic nature of climate) and forced (related to changes in forcings) variability but it is still unclear to what extent human activities are responsible for these changes. We used a statistical method to distinguish between changes caused by humans and by natural influences both for instrumental observations and reconstructions of past climate. Our results show that the observed changes since the 1950s are out of the range of natural variability and can be attributed to human activities – i.e., the increase of greenhouse gases and stratospheric ozone depletion. Therefore, our findings indicate that the future state of the West Antarctic surface climate will depend on the greenhouse gas emissions as well as the ozone layer recovery.

1 Introduction

Over the past decades, the Antarctic has experienced large climate changes, in particular over the West Antarctic Ice Sheet (WAIS), situated in the Pacific Sector of the Southern Ocean (e.g., IPCC, 2019). The widespread atmospheric warming observed (e.g.,

Steig et al., 2009) there is associated with a snow accumulation increase over the Antarctic Peninsula, Eastern and Central WAIS, and a snow accumulation decrease in Western WAIS (Medley & Thomas, 2019). It has been shown that these changes are closely related to modifications in the general atmospheric circulation (e.g., Marshall & Thompson, 2016; Marshall et al., 2017; Thomas et al., 2015; Medley & Thomas, 2019; Dalaiden et al., 2021), and in particular in the low-pressure system situated off the West Antarctic coasts, referred to as the Amundsen Sea Low (ASL) (Turner et al., 2009; Raphael et al., 2016; Hosking et al., 2013). Given the critical importance of the West Antarctic climate variability on the future global climate, better understanding the drivers of these surface changes as well as the contribution from the forced and internal variability is crucial for reducing uncertainties in climate projections.

Stratospheric ozone depletion has been identified as the main contributor to the atmospheric circulation changes in the Southern Hemisphere, with a minor contribution from the increase in greenhouse gas concentrations (Thompson et al., 2011; England et al., 2016; Fogt & Zbacnik, 2014). Additionally, stratospheric ozone depletion may account for almost a third of the modelled Antarctic-wide snow accumulation increase over 1986–2005 (Lenaerts et al., 2018). Furthermore, the widespread post-1950s West Antarctic atmospheric warming strongly suggests an important role of greenhouse gases (Steig et al., 2009). Similarly, according to Medley and Thomas (2019), the overall warming of the atmosphere may explain the 20th century Antarctic-wide snow accumulation. In addition to the Gillett et al. (2008) study which attributed warming at both poles to anthropogenic forcing, two recent studies (Swart et al., 2018; Hobbs et al., 2021) have demonstrated that the observed warming and freshening of the Southern Ocean since the 20th century are inconsistent with internal variability of the climate alone and is mainly attributed to the increased atmospheric greenhouse gas concentrations and ozone depletion. Furthermore, the summer austral increase of the Southern Annular Mode (roughly representing the position and intensity of the westerly winds (Fogt & Marshall, 2020)) since the 1950s is one of the unique atmospheric changes that has been attributed to a forcing (Gillett et al., 2013; Jones et al., 2016). However, to our knowledge, no optimal fingerprinting study exists of the ASL changes, and more generally of the West Antarctic climate changes over the past decades.

This can be explained by the very sparse observational network (Turner et al., 2005) and the strong internal climate variability in the West Antarctic (e.g., Connolley, 1997)

that make it complicated to detect a forced trend. However, over the past years, several spatially complete datasets have been released describing the atmospheric circulation (Fogt et al., 2019; Dalaiden et al., 2021; O'Connor et al., 2021), atmospheric temperature (Nicolas & Bromwich, 2014) and snow accumulation (Medley & Thomas, 2019; Dalaiden et al., 2021) in this region. In parallel, large ensembles (LEs) of Earth System Model (ESM) simulations are becoming more common (Deser, Lehner, et al., 2020; Maher et al., 2021). Single model LEs are built by performing several simulations with a single climate model using the same forcing but initialized with slightly different initial conditions to estimate the effect of internal variability. As a consequence, LEs allow comparing the contribution from the internal and forced variability on the simulated changes. LEs are particularly relevant for detection and attribution studies since the impact of unpredictable internal variability is minimized with the average of the simulations (i.e., maximising the signal-to-noise ratio). Additionally, some LEs provide single-forcing experiments, which provide the opportunity to assess the impact of a specific forcing.

In this study, we aim at detecting and attributing the forced response of the atmospheric circulation, near-surface air temperature and snow accumulation in the West Antarctic over the past decades, and, second, at isolating the individual contributions from the greenhouse gas increase and stratospheric ozone depletion on the climate changes. To this end, we perform a detection and attribution analysis (D&A), in order to separate the observed climate changes into two components: a component related to internal variability of the climate system, and another related to changes in the anthropogenic and natural forcings (Hegerl & Zwiers, 2011). This allows us to assess the anthropogenic influence on the ongoing surface climate changes occurring in the West Antarctic since the mid-20th century. To do so, we employ new existing instrumental and proxy-based reconstructions and two LEs of ESM simulations.

2 Methods

2.1 Observations and reconstructions

Although some atmospheric pressure observations span the past century, the vast majority start at best in 1958 (Turner et al., 2004). To put the recent changes in a broader context and identify the potential long-term effect of the forcing, we thus need to rely on reconstructions based on paleo proxies (for instance ice core data), which provide ro-

bust sea-level pressure reconstructions over the past few centuries. In this study, we use the sea-level pressure reconstruction covering the 1800–2000 CE time period from Dalaiden et al. (2021) who dynamically constrain the climate evolution in the West Antarctic sector with ice core snow accumulation and isotopic content proxy data along with tree ring width records within a data assimilation framework. When compared with observations over the satellite era, this reconstruction shows good skill (Dalaiden et al., 2021; O'Connor et al., 2021). For near-surface air temperature, the instrumental-based reconstruction from Nicolas and Bromwich (2014) that spans the 1958–2012 CE time period is employed. This reconstruction shows a good agreement with independent observations and is considered as the reference temperature reconstruction for the second half of the 20th century. Finally, for snow accumulation, we use the well-evaluated reconstruction of Medley and Thomas (2019), which uses the combination of ice core snow accumulation records with atmospheric reanalysis to ensure spatial coherence.

2.2 Climate model simulations

LEs are ideal for detection and attribution studies as a large number of model simulations is required to reduce the noise associated with internal variability. In this study, we use two LEs performed with two different ESMs, which also include several additional experiments driven by different forcing combinations. The first LE has been performed with the Coupled Earth System Model version 1 (CESM1) (Kay et al., 2015). CESM1-LE consists of 35 ensemble members covering the 1920–2080 CE period and are driven by the historical forcing until 2005 CE and the Representative Concentration Pathway (RCP) 8.5 afterwards (CMIP5 forcings). In addition to the 35 historical ensemble members, Deser, Phillips, et al. (2020) conducted additional experiments of 20 ensemble members to isolate the impacts of GHG and anthropogenic aerosols (AER). More specifically, these two specific-forcing LEs follow the same protocol as for the historical LE but the forcing (i.e., the greenhouse gases or anthropogenic aerosols) is set at the 1920 CE level throughout the simulation (i.e., all-but-one-forcing). These two ensembles are referred to as xGHG and xAER, respectively. Along with these two all-but-one-forcing LEs, Landrum et al. (2017) provided an ensemble of eight ensemble members following the same protocol as xGHG and xAER but with the stratospheric ozone concentration fixed at the 1955 CE level (referred to as xO3). For deriving the GHG, O3 and AER ensembles from the ALL, xGHG, xAER and xO3 ensembles, we follow the procedure of Deser, Phillips,

et al. (2020). Numerous studies have shown that CESM1 simulates relatively well the climate around the Antarctic when compared with regional climate models and observations (e.g., Lenaerts et al., 2016; Dalaiden et al., 2021; England et al., 2016; Landrum et al., 2017), which gives confidence in the use of CESM1 for this study.

In addition to CESM1, we also employ a second LE performed with the ESM CanESM2 (Arora et al., 2011; Kirchmeier-Young et al., 2017). This LE is available over 1950–2100 CE. This LE contains four experiments of 50 ensemble members with different forcings. As in the case of CESM1, an experiment driven by the historical forcing from 1950 until 2005 CE and by the RCP8.5 forcing from 2005 CE is available. The three other experiments consist of single-forcing experiments: natural (solar and volcanic forcings; NAT), AER and O3. In contrast with CESM1, the single-forcing experiments are performed by keeping all the forcings constant except the forcing of interest throughout the simulation. As in Swart et al. (2018), we estimate the response to the anthropogenic greenhouse gases by subtracting the responses of all of the single-forcing experiments from the response of the experiment with all forcings. Although CanESM2 has been less analyzed than CESM1 in the Antarctic, this model has been recently used to identify the forced drivers of the surface changes in the Southern Ocean over the 20th century (Swart et al., 2018; Hobbs et al., 2021).

2.3 Detection and attributions analysis

We first associate the evolution of a climate variable with a specific forcing by comparing the trends over the past decades in the all-forcing experiment (ALL) and a single-forcing experiment. This simple analysis allows us to give a first estimate of the role of a specific forcing on the total simulated response. In addition, we conduct a D&A analysis (Ribes & Terray, 2013) on the atmospheric circulation, surface air temperature and snow accumulation in the West Antarctic sector over the 1950 CE post period. As per Hegerl and Zwiers (2011), we consider that the detection is successful when the observed change is outside of the range of internal variability of the climate system and the attribution as assigning a change to a specific forcing. The method used in thus study is detailed in Section S1 (Supporting Information).

The D&A analysis is performed on the ASL index (computed as the average sea-level pressure over 170–290°E, 75–60°S as in Hosking et al. (2013)), West Antarctic near-

surface air temperature and snow accumulation. For temperature and snow accumulation, the four regional time-series (see Figure S1 for the definitions of the regions) are included in the regression to increase the probability to detect a change by including the spatial component. The analysis period is 1950–2000 CE for the ASL and snow accumulation, and 1959–2012 CE for temperature. These periods reflect the periods covered by both the observations and climate model simulations.

3 Results

3.1 Observed and simulated surface climate changes since the mid-20th century

Figure 1 a shows the annual evolution of the ASL index in the proxy-based reconstruction of Dalaiden et al. (2021) and as simulated in CESM1-LE and CanESM2-LE over 1950–2080 CE. Both the reconstruction and climate model simulations display a deepening of the ASL over the second half of the 20th century, which is consistent with previous studies (Thomas et al., 2015; Dalaiden et al., 2021; O'Connor et al., 2021). The reconstructed trend over 1951–2000 CE is in the range of the simulated trends (Figure 1 b; -0.40 hPa per decade vs -0.26 $\pm$ 0.18 hPa per decade (mean $\pm$ std) and -0.30 $\pm$ 0.17 hPa per decade for CESM1-LE and CanESM2-LE, respectively; all statistically significant at the 95% level). Both CESM1-LE and CanESM2-LE suggest a further deepening of the ASL for the end of the 21st century but at a lower rate: -0.22 $\pm$ 0.16 hPa per decade and -0.18 $\pm$ 0.14 hPa per decade over 2031–2080 CE, respectively.

Figure 2 presents maps of the observed linear trends of sea-level pressure, near-surface air temperature and snow accumulation along with the forced response from the ALL experiment for CESM1-LE and CanESM2-LE over 1959–2000 CE. While the reconstruction shows a deepening of the ASL and an increased anticyclonic situation around the Drake Passage and Weddell Sea, the deepening of the ASL present in the total forced trend from the two models is rather embedded in a Southern Annular Mode (SAM)-dominated response (i.e., observations are more zonally asymmetric than the forced response). This is not a contradictory result since the ensemble mean is dominated by the forced response with the internal variability reduced (by averaging over the ensemble members). Indeed, some ensemble members display a pattern similar to the reconstruction (Figures S1 and S2). We therefore argue that the difference in the trend between the reconstruction and

ensemble means mainly comes from the contribution of internal variability present in the reconstruction but that is reduced in the model ensemble means.

The signal observed in the near-surface air temperature over 1959–2000 CE is characterized by a large warming over the Antarctic Peninsula (0.35°C decade^{-1} [p-value<0.05]) and the Central WAIS (0.31°C decade^{-1} [p-value<0.05]; Figure 2 and Table S1; see Figure S1 for the definitions of the regions). The forced response of the ALL experiment displays a more homogeneous surface warming pattern, albeit both CESM1-LE and CanESM2-LE show the strongest warming in the Antarctic Peninsula (0.21 °C decade^{-1} [p-value<0.05] and 0.35 °C decade^{-1} [p-value<0.05], respectively) and underestimate the warming in the Central WAIS (0.11°C decade^{-1} [p-value<0.05] and 0.16°C decade^{-1} [p-value<0.05], respectively). Finally, we observe a good agreement between observed and forced simulated snow accumulation changes over 1959–2000 CE (Figure 2). Both the Medley and Thomas (2019) reconstruction and models display a snow accumulation increase over the Antarctic Peninsula, and the Eastern and Central WAIS: for those three regions taken together the observations give a trend of 35.22 Gt decade^{-1} against 14.86 Gt decade^{-1} for CESM1-LE and 11.95 Gt decade^{-1} for CanESM2-LE (all statistically significant at the 95% level). For Western WAIS, a statistically significant snow accumulation decrease is observed (-9.29 Gt decade^{-1}), in contrast with the two models that show no significant change (Table S1). For both temperature and snow accumulation, some ensemble members are in better agreement with the reconstruction (especially regarding the magnitude of change; Figures S4-S7) indicating a substantial role of internal variability in the observed changes.

3.2 Detection and attribution to individual forcings

Figure 3 presents the contribution of the increased greenhouse gas and stratospheric ozone depletion to the sea-level pressure, near-surface air temperature and snow accumulation trends from CESM1-LE and CanESM2-LE over 1959–2000 CE. Stratospheric ozone depletion and greenhouse gases are the main drivers of the deepening ASL over 1959–2000 CE in both models, since the forced trend patterns of sea-level pressure from these two forcings are very similar to the total forced trend pattern (Figure 3). The stratospheric ozone depletion experiments display a -0.25 hPa decade^{-1} (p-values<0.01) and -0.16 hPa decade^{-1} (p-values<0.01) trend for CESM1-LE and CanESM2-LE respectively, while the greenhouse gases experiments show -0.18 hPa decade^{-1} (p-values<0.01) and

-0.19 hPa decade^{-1} (p-values<0.01) trend for CESM1-LE and CanESM2-LE respectively (Table S1).

In contrast with the atmospheric circulation, the greenhouse gas forcing explains most of the total forced pattern of the near-surface air temperature trend over 1959–2000 CE (Figure 3) while the stratospheric ozone depletion forcing is associated with no statistically significant surface temperature changes for West Antarctica in both models (Table S1). However, it is worth noting that the stratospheric ozone depletion forcing leads to surface warming in the Antarctic Peninsula (Table S1). Furthermore, the GHG spatial pattern of trends in near-surface air temperature is relatively homogeneous compared with the O3 spatial pattern (Figure 3). As for snow accumulation, our analysis indicates that both the greenhouse gases and stratospheric ozone depletion are responsible for the observed snow accumulation changes (Figure 3). Furthermore, in the two models, the spatial fingerprint of the stratospheric ozone depletion forcing on the snow accumulation trends is more heterogeneous than the one related to the greenhouse gas forcing. The former is associated with more pronounced trends that are in opposition between the Antarctic Peninsula, Eastern and Central WAIS, and the Western WAIS. This pattern is typically related to the influence of the ASL (Dalaiden et al., 2021) and therefore explains the substantial role of stratospheric ozone depletion on the snow accumulation changes.

Results from the formal D&A analysis (section 2.3) are displayed in Figure 4. Both CESM1-LE and CanESM2-LE show that an impact of all forcings on changes in the ASL, near-surface air temperature and snow accumulation over the past decades is detected, since the scaling factors (including the confidence intervals) are different from zero (Figure 4). The observed changes cannot be thus explained by internal variability. Therefore, according to our results, changes in the forcings are responsible for the recent surface climate changes in the West Antarctic. It is worth noting that the confidence intervals are the largest for the ASL. This could suggest that, although the impact of the forcings on the ASL is detected, internal variability plays an important role in the ASL variability compared with the other two variables.

Regarding the attribution to specific forcings, both models show a detectable response to the greenhouse gas forcing for near-surface air temperature and snow accumulation, since the scaling factors are different from zero (Figure 4). In contrast with CESM1-

LE, the greenhouse gas forcing is also detected for the ASL in CanESM2-LE. However, when extending the period to 1940–2000 CE, results from CESM1-LE also display a detection of the greenhouse gas forcing on the ASL (not shown). In addition to the greenhouse gas forcing, CESM1-LE indicates that the impact of stratospheric ozone depletion on the ASL and snow accumulation is also detectable. The scaling factor is relatively high, which could be explained by the fact that stratospheric ozone depletion is not dominant all year long but primarily during the austral summer (Thompson et al., 2011). Regarding near-surface air temperature, the scaling factor for stratospheric ozone depletion is statistically different from zero. However, the high scaling factor value suggests that, while the observed pattern resembles the ozone signal, the amplitude of the simulated signal is too small to confidently attribute it to this forcing. Finally, according to CanESM2-LE results, the natural forcing (probably volcanic eruptions) is also detected in temperature and snow accumulation changes. For all the analyzed variables, the ALL forcings results show clear detection of a forced signal (since scaling factors generally include unity), but the attribution to a specific forcing is less clear.

4 Discussion and conclusions

Our results are directly impacted by several sources of uncertainties. Since we use the D&A analysis to detect forced signal in the observed time-series, any errors in that time-series may impact the scaling factors, and therefore potentially our ability to detect and attribute the observed changes. Yet, the observational network is sparse in Antarctica. For instance, the instrumental-based near-surface air temperature reconstruction of Nicolas and Bromwich (2014) is only based on four records situated in West Antarctica. Additionally, for the ASL and snow accumulation, we had to rely on the reconstructions based on paleo records, which are known to be more prone to uncertainties than instrumental records. Although the information on the uncertainty is available, directly considering account it in the D&A framework is challenging. However, we note that these proxy-based reconstructions are well evaluated against state-of-the-art observations (Dalaiden et al., 2021; Medley & Thomas, 2019), which thus gives confidence in our results. Furthermore, the estimations of the forced responses depend on the climate model, and therefore the model biases may impact the conclusions. However, here, we have analyzed two models developed by two different groups from which we generally obtained the same conclusions.

While considering these limitations, our results robustly show that the annual deepening of the ASL, surface warming and snow accumulation increase in West Antarctica since the 1950s are out of the range of internal variability and can be attributed to the anthropogenic forcing. In agreement with previous studies that concluded for a forced response of the ASL during the austral summer due to anthropogenic forcing, and in particular to stratospheric ozone depletion over about 1965–2005 CE (England et al., 2016; Fogt & Zbacnik, 2014), we argue that the deepening ASL over 1950–2000 CE can be only explained on the annual basis by changes in the forcings. Furthermore, as for near-surface air temperature, a previous study (i.e., Smith & Polvani, 2017) found that the West Antarctic surface warming over the past decades is not out of the range of internal variability. However, we argue that our findings are not in contradiction with their results. Smith and Polvani (2017) focused on the 1960–2005 CE period, while our analysis is performed on a longer period (i.e., 1959–2012 CE). According to Smith and Polvani (2017), a forced anthropogenic signal emerges when analyzing temperature changes over a longer period. The probability density distributions of the 46-year and 54-year temperature trends from the control pre-industrial simulation of CESM1 (Figure S8) indicate that the observed 1959–2012 CE temperature trend is out of the range of internal variability (>99.9th percentile), in contrast with the 1960–2005 CE trend (<99.9th percentile). Additionally, Smith and Polvani (2017) analyzed all available model simulations, regardless of their performance in simulating the Antarctic climate and did not use an optimal fingerprinting method, which would have better handled the role of internal variability on observed changes (similar conclusions are obtained with CanESM2 [Figure S9]). Finally, the detection of surface warming is consistent with the findings of Gillett et al. (2008) who showed that the atmospheric warming at the two poles is due to human activities.

The detection of snow accumulation changes is less robust than for temperature and ASL since the scaling factors including confidence intervals are greater than unity, especially for CanESM2-LE. This means that the models underestimate the amplitude of change. Unlike sea-level pressure and temperature, snow accumulation strongly varies in space, making a successful detection more challenging. The coarse resolution of the ESMs – which fails to represent small spatial scale processes –, missing processes in ESMs along with the uncertainties in ice core records are likely to blame. However, Medley and Thomas (2019) showed that 80% of the variance in spatial snow accumulation trends over 1957–2000 CE are explained by the positive SAM trend – yet the ASL is strongly related

to the SAM (Turner et al., 2009; Hosking et al., 2013). Furthermore, the general atmospheric warming may be the primary driver of the 20th century Antarctic snow accumulation increase (Medley & Thomas, 2019; Dalaiden et al., 2020). Since changes in the ASL and temperature can be attributed to forcings according to our results and previous studies (England et al., 2016; Fogt & Zbacnik, 2014; Gillett et al., 2008), we believe that our snow accumulation results are not an artefact.

Both CESM1-LE and CanESM2-LE agree on the important role of the greenhouse gas forcing on these changes occurring in the West Antarctic. The detection of the greenhouse gas forcing on those climate changes can be related to physical mechanisms highlighted in previous studies. Higher greenhouse gas concentrations strengthen the temperature gradient between the mid and high latitudes, which results in intensifying the westerly jet (e.g., Arblaster & Meehl, 2006), and therefore the deepening ASL (e.g., Fogt & Marshall, 2020). Yet, the ASL strongly modulates the surface climate in West Antarctica (e.g., Raphael et al., 2016) by enhancing the southerly flow towards the Eastern WAIS and Antarctic Peninsula, including the intrusions of moist and warm air in these regions. In contrast, the Western WAIS is less prone to these intrusions for years with strong ASL (Fogt et al., 2012; Fyke et al., 2017). This results in surface warming in Eastern WAIS and the Antarctic Peninsula, and surface cooling in the Western WAIS (Marshall & Thompson, 2016). Over the Antarctic Peninsula and Eastern and Central WAIS, an overall positive correlation between atmospheric temperature and snow accumulation is noticed (Cavitte et al., 2020). In these regions, when warm, moist air from the ocean is brought to the continent by the ASL, air moisture content precipitates due to the orographic lifting, leading to more snow accumulation in these regions. Because the air has lost almost all of its humidity content during adiabatic uplift, Western WAIS experiences a snow accumulation deficit due to the ASL deepening, strengthening the Eastern/Western snow accumulation dipole (Dalaiden et al., 2021). Furthermore, the greenhouse gas forcing leads to a uniform surface warming, which agrees with Bindoff et al. (2013). This explains, for instance, the surface warming observed in the Central and Western WAIS that cannot be explained by the ASL deepening.

Furthermore, our results based on CESM1-LE indicate that stratospheric ozone depletion is the primary driver of the deepening ASL over the second half of the 20th century (followed by the greenhouse gas forcing). This forcing impacts the atmospheric circulation without destabilizing the global energy budget directly (Thompson et al., 2011),

in contrast with the greenhouse gas forcing. By primarily modifying wind patterns, partly through the ASL, stratospheric ozone depletion leads to a more pronounced dipole between the Western WAIS/Antarctic Peninsula and the Eastern WAIS for both near-surface air temperature and snow accumulation. Therefore, we confirm previous findings on the major role of this forcing on the recent snow accumulation increase (Lenaerts et al., 2018; Chemke et al., 2020) and more generally on the ASL (England et al., 2016; Fogt & Zbacnik, 2014). In contrast with these studies, we formally performed a D&A analysis to analyze the forced response to the stratospheric ozone depletion. It worth noting that the role of stratospheric ozone depletion in CanESM2 is less clear than in CESM1 since only the greenhouse gas forcing is detected in the D&A analysis. However, the forced atmospheric circulation changes associated with stratospheric ozone depletion in CanESM2 suggests a substantial contribution from this forcing.

In summary, our study shows that the overall observed ASL, near-surface air temperature and, with slightly lower confidence, snow accumulation changes over the past decades can be attributed to the greenhouse gas and, in some cases, stratospheric ozone depletion forcings. Therefore, we could expect that these changes will continue in the coming decades because of the increasing greenhouse gas concentrations. However, thanks to the Montreal Protocol (Kuttippurath & Nair, 2017) aiming to decrease the substances responsible for stratospheric ozone depletion, the recovery of the stratospheric ozone layer could mitigate the impact of the greenhouse gas forcing. The ozone recovery would lead to a more anticyclonic situation in the West Antarctic (i.e., decreased deepening ASL). As a weaker ASL tends to reduce glacier thinning (Dotto et al., 2020), this atmospheric situation could have major implications for the global sea-level rise by decreasing the contribution of the Antarctic Ice Sheet.

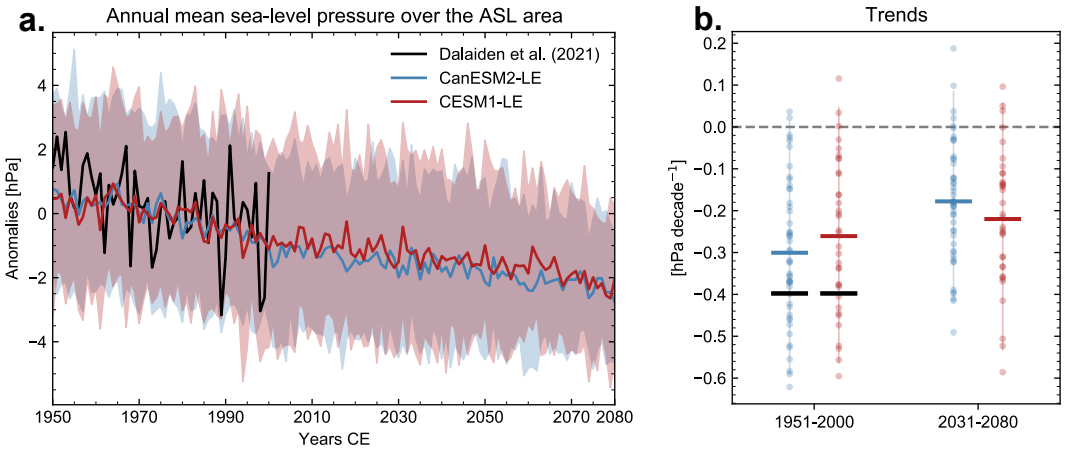

Figure 1. (**a**) Annual reconstructed (i.e., Dalaiden et al. (2021)) and simulated (CESM1-LE and CanESM2-LE) sea-level pressure over the Amundsen Sea Low area (in hPa) over 1950–2080 CE. The shaded areas correspond to the 5th and 95th percentiles of the model ensemble. (**b**) Linear trends over the 1951–2000 CE and 2031–2080 CE periods are displayed. The color dots correspond to the trend for each ensemble member and the horizontal thick coloured line corresponds to the ensemble mean. The horizontal thick black line is the observed trend.

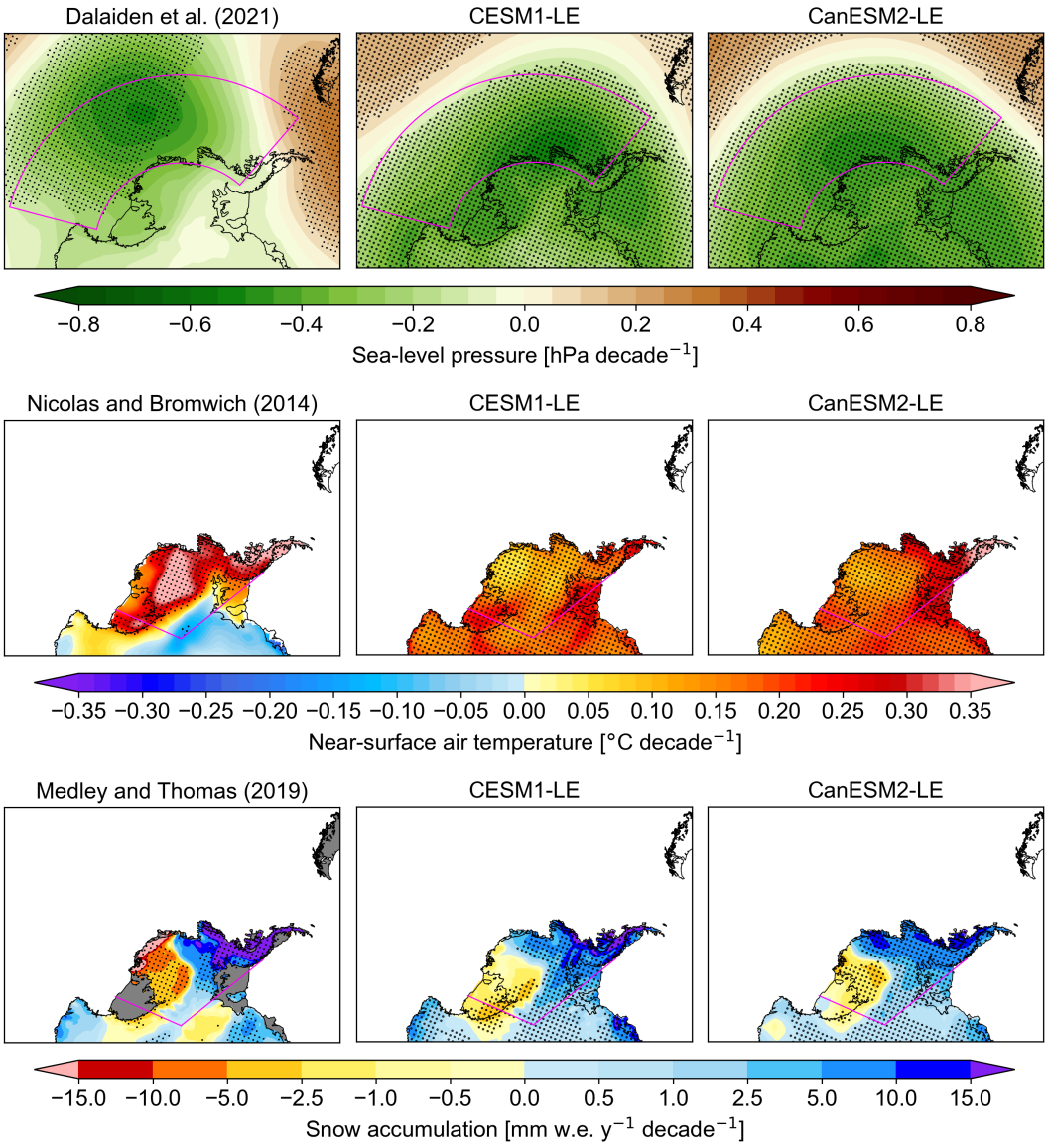

Figure 2. Reconstructed and simulated (CESM1-LE and CanESM2-LE) linear trends in sea-level pressure (hPa decade^{-1}), near-surface air temperature (°C decade^{-1}) and snow accumulation (mm w.e. y^{-1} decade^{-1}) over 1959–2000 CE. The reconstructed sea-level pressure corresponds to the paleo-based reconstruction of Dalaiden et al. (2021), while for snow accumulation, the ice core-based reconstruction of Medley and Thomas (2019) is displayed. The near-surface air temperature reconstruction is from the reconstruction of Nicolas and Bromwich (2014), which is based on instrumental records. The simulated trends correspond to the ensemble mean of the CESM1-LE and CanESM2-LE all forcing experiments (30 and 50 ensemble members, respectively). Stippling indicates statistical significant trends (95% confidence). For sea-level pressure, the magenta box corresponds to the area on which the Amundsen Sea Low index is computed. Magenta lines displayed in near-surface air temperature and snow accumulation maps correspond to the limits of West Antarctica.

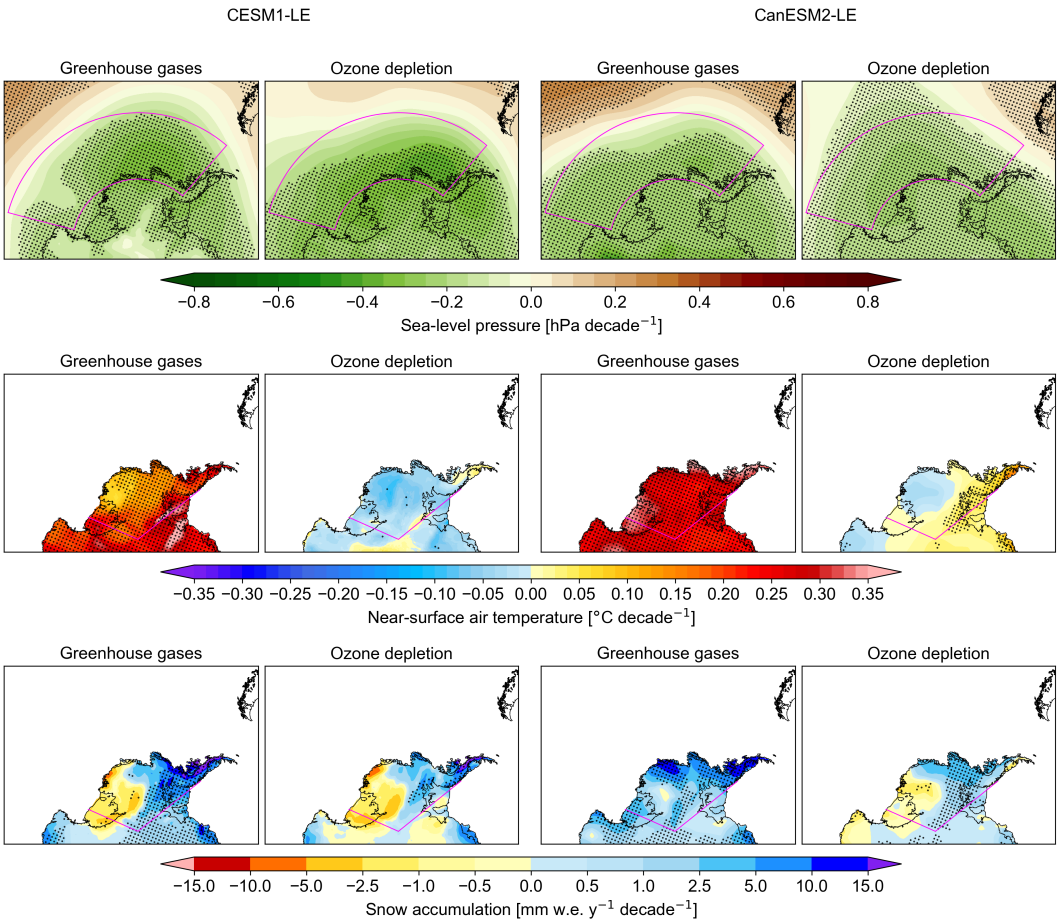

Figure 3. Annual linear trends for sea-level pressure (hPa decade^{-1}), near-surface air temperature (°C decade^{-1}) and snow accumulation (mm w.e. y^{-1} decade^{-1}) from the ensemble mean greenhouse gases and ozone depletion experiments performed with CESM1 and CanESM2 over 1959–2000 CE. Stippling indicates statistically significant trends at 95% level. For sea-level pressure, the magenta box corresponds to the area on which the Amundsen Sea Low index is computed. Magenta lines displayed in near-surface air temperature and snow accumulation maps correspond to the limits of West Antarctica.

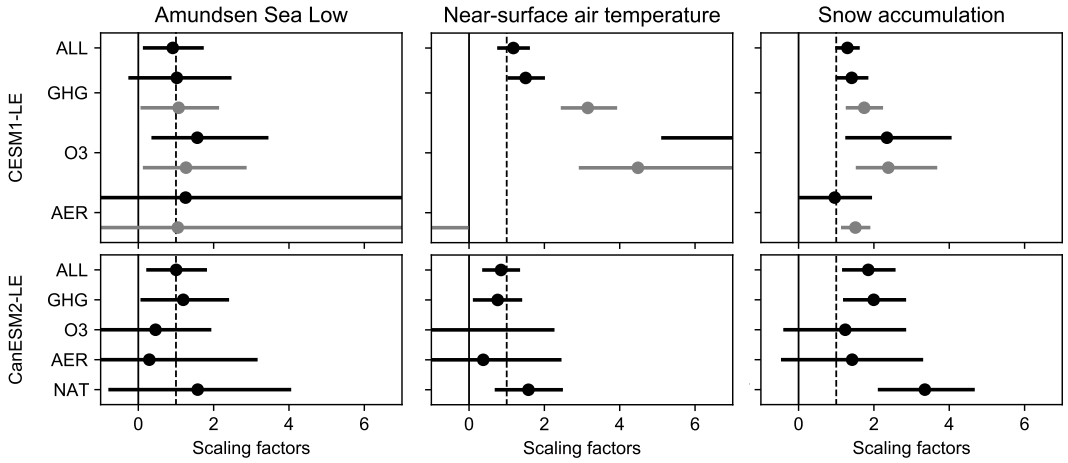

Figure 4. Detection and attribution scaling factors for the mean sea-level pressure over the Amundsen Sea Low area over 1950–2000 CE, near-surface air temperature over 1959–2012 CE and snow accumulation over 1950–2000 CE in West Antarctica for CESM1-LE (top) and canESM2-LE (bottom). The ASL proxy-based reconstructions of (Dalaiden et al., 2021) and the snow accumulation proxy-based reconstruction of (Medley & Thomas, 2019) are used as observations in the D&A analysis while the instrumental-based reconstruction of (Nicolas & Bromwich, 2014) is used for near-surface air temperature. As for CESM1-LE, the scaling factors for GHG, O3 and AER are displayed in black and the scaling factors for all-but-the specific forcing are shown in grey. Due to model output availability, the D&A analysis using the stratospheric ozone depletion ensemble of CESM1 is performed over 1955–2000 CE for the ASL and snow accumulation, and 1959–2005 CE for near-surface air temperature. Error bars correspond to the 90% confidence intervals. All the data are annual averages.

5 Data Availability Statement

The near-surface air temperature reconstruction of Nicolas and Bromwich (2014) can be downloaded at `http://polarmet.osu.edu/datasets/Antarctic_recon/`. The paleo snow accumulation reconstruction of Medley and Thomas (2019) is available at `https://earth.gsfc.nasa.gov/cryo/data/antarctic-accumulation-reconstructions` while the reconstruction of the atmospheric circulation from Dalaiden et al. (2021) is archived on Zenodo (`https://zenodo.org/record/4770179#.YmbEtC8Rr0o`). The CESM1 and CanESM2 data used in this study are freely available through `https://www.earthsystemgrid.org` and `https://data-donnees.ec.gc.ca`, respectively.

Acknowledgments

We thank William Hobbs and an anonymous reviewer for their constructive comments, which greatly helped to improve our manuscript. QD is a Research Fellow within the F.R.S.-FNRS (Belgium). G.H. and A.S. were funded by the NERC project GloSAT (NE/S015698/1). A.S. further received funding from a Chancellors fellowship at the University of Edinburgh. HG is a Research Director within the F.R.S.-FNRS (Belgium). This work was partly supported by the Belgian Research Action through Interdisciplinary Networks (BRAIN-be) from the Belgian Science Policy Office in the framework of the project "East Antarctic surface mass balance in the Anthropocene: observations and multiscale modelling (Mass2Ant)" (contract no. BR/165/A2/Mass2Ant).

References

Arblaster, J. M., & Meehl, G. A. (2006). Contributions of external forcings to southern annular mode trends. *Journal of Climate*, *19*(12), 2896–2905. doi: 10.1175/JCLI3774.1

Arora, V. K., Scinocca, J. F., Boer, G. J., Christian, J. R., Denman, K. L., Flato, G. M., ... Merryfield, W. J. (2011). Carbon emission limits required to satisfy future representative concentration pathways of greenhouse gases. *Geophysical Research Letters*, *38*(5), 3–8. doi: 10.1029/2010GL046270

Bindoff, N. L., Stott, P. A., AchutaRao, K. M., Allen, M. R., Gillett, N., Gutzler, D., ... Zhang, X. (2013). Detection and attribution of climate change: From global to regional. In T. F. Stocker et al. (Eds.), *Climate change 2013: The physical science basis. contribution of working group i*

to the fifth assessment report of the intergovernmental panel on climate change (pp. 867–952). Cambridge, UK: Cambridge University Press. doi: 10.1017/CBO9781107415324.022

Cavitte, M., Dalaiden, Q., Goosse, H., Lenaerts, J., & Thomas, E. (2020). Reconciling the surface temperature–surface mass balance relationship in models and ice cores in Antarctica over the last two centuries. *The Cryosphere*, *14*, 4083–4102. doi: 10.5194/tc-2020-36

Chemke, R., Previdi, M., England, M. R., & Polvani, L. M. (2020). Distinguishing the impacts of ozone and ozone-depleting substances on the recent increase in Antarctic surface mass balance. *Cryosphere*, *14*(11), 4135–4144. doi: 10.5194/tc-14-4135-2020

Connolley, W. M. (1997). Variability in annual mean circulation in southern high latitudes. *Climate Dynamics*, *13*(10), 745–756. doi: 10.1007/s003820050195

Dalaiden, Q., Goosse, H., Lenaerts, J. T., Cavitte, M. G., & Henderson, N. (2020). Future Antarctic snow accumulation trend is dominated by atmospheric synoptic-scale events. *Communications Earth & Environment*, *1*, 1–9. Retrieved from `http://dx.doi.org/10.1038/s43247-020-00062-x` doi: 10.1038/s43247-020-00062-x

Dalaiden, Q., Goosse, H., Rezsöhazy, J., & Thomas, E. R. (2021). Reconstructing atmospheric circulation and sea-ice extent in the west antarctic over the past 200 years using data assimilation. *Climate Dynamics*, *57*(11), 3479–3503. Retrieved from `https://doi.org/10.1007/s00382-021-05879-6` doi: 10.1007/s00382-021-05879-6

Deser, C., Lehner, F., Rodgers, K. B., Ault, T., Delworth, T. L., DiNezio, P. N., ... Ting, M. (2020). Insights from Earth system model initial-condition large ensembles and future prospects. *Nature Climate Change*, *10*(4), 277–286. Retrieved from `http://dx.doi.org/10.1038/s41558-020-0731-2` doi: 10.1038/s41558-020-0731-2

Deser, C., Phillips, A. S., Simpson, I. R., Rosenbloom, N., Coleman, D., Lehner, F., ... Stevenson, S. (2020). Isolating the evolving contributions of anthropogenic aerosols and greenhouse gases: A new CESM1 large ensemble community resource. *Journal of Climate*, *33*(18), 7835–7858. doi: 10.1175/JCLI-D-20-0123.1

Dotto, T. S., Naveira Garabato, A. C., Wåhlin, A. K., Bacon, S., Holland, P. R., Kimura, S., ... Jenkins, A. (2020). Control of the Oceanic Heat Content of the Getz-Dotson Trough, Antarctica, by the Amundsen Sea Low. *Journal of Geophysical Research: Oceans*, *125*(8). Retrieved from `https://doi.org/10.1029/2020JC016113` doi: 10.1029/2020JC016113

England, M. R., Polvani, L. M., Smith, K. L., Landrum, L., & Holland, M. M. (2016). Robust response of the Amundsen Sea Low to stratospheric ozone depletion. *Geophysical Research Letters*, *43*(15), 8207–8213. doi: 10.1002/2016GL070055

Fogt, R. L., & Marshall, G. J. (2020). The Southern Annular Mode: Variability, trends, and climate impacts across the Southern Hemisphere. *WIREs Climate Change*, *n/a*(n/a), e652. Retrieved from `https://doi.org/10.1002/wcc.652` doi: 10.1002/wcc.652

Fogt, R. L., Schneider, D. P., Goergens, C. A., Jones, J. M., Clark, L. N., & Garberoglio, M. J. (2019). Seasonal Antarctic pressure variability during the twentieth century from spatially complete reconstructions and CAM5 simulations. *Climate Dynamics*, *53*(3), 1435–1452. Retrieved from `http://dx.doi.org/10.1007/s00382-019-04674-8` doi: 10.1007/s00382-019-04674-8

Fogt, R. L., Wovrosh, A. J., Langen, R. A., & Simmonds, I. (2012). The characteristic variability and connection to the underlying synoptic activity of the Amundsen-Bellingshausen Seas Low. *Journal of Geophysical Research Atmospheres*, *117*(7), 1–22. doi: 10.1029/2011JD017337

Fogt, R. L., & Zbacnik, E. A. (2014). Sensitivity of the Amundsen sea low to stratospheric ozone depletion. *Journal of Climate*, *27*(24), 9383–9400. doi: 10.1175/JCLI-D-13-00657.1

Fyke, J., Lenaerts, J. T., & Wang, H. (2017). Basin-scale heterogeneity in Antarctic precipitation and its impact on surface mass variability. *Cryosphere*, *11*(6), 2595–2609. doi: 10.5194/tc-11-2595-2017

Gillett, N. P., Arora, V. K., Matthews, D., & Allen, M. R. (2013). Constraining the ratio of global warming to cumulative CO2 emissions using CMIP5 simulations. *Journal of Climate*, *26*(18), 6844–6858. doi: 10.1175/JCLI-D-12-00476.1

Gillett, N. P., Stone, D. A., Stott, P. A., Nozawa, T., Karpechko, A. Y., Hegerl,

G. C., ... Jones, P. D. (2008). Attribution of polar warming to human influence. *Nature Geoscience*, *1*(11), 750–754. doi: 10.1038/ngeo338

Hegerl, G., & Zwiers, F. (2011). Use of models in detection and attribution of climate change. *Wiley Interdisciplinary Reviews: Climate Change*, *2*(4), 570–591. doi: 10.1002/wcc.121

Hobbs, W. R., Roach, C., Roy, T., Sallée, J.-B., & Bindoff, N. (2021). Anthropogenic temperature and salinity changes in the southern ocean. *Journal of Climate*, *34*(1), 215 - 228. Retrieved from `https://journals.ametsoc.org/view/journals/clim/34/1/jcliD200454.xml` doi: 10.1175/JCLI-D-20-0454.1

Hosking, J. S., Orr, A., Marshall, G. J., Turner, J., & Phillips, T. (2013). The influence of the amundsen-bellingshausen seas low on the climate of West Antarctica and its representation in coupled climate model simulations. *Journal of Climate*, *26*(17), 6633–6648. doi: 10.1175/JCLI-D-12-00813.1

IPCC. (2019). IPCC Special Report on the Ocean and Cryosphere in a Changing Climate [H.-O. Pörtner, D.C. Roberts, V. Masson-Delmotte, P. Zhai, M. Tignor, E. Poloczanska, K. Mintenbeck, A. Alegría, M. Nicolai, A. Okem, J. Petzold, B. Rama, N.M. Weyer (eds.)]. *In press*.

Jones, J. M., Gille, S. T., Goosse, H., Abram, N. J., Canziani, P. O., Charman, D. J., ... Vance, T. R. (2016). Assessing recent trends in high-latitude Southern Hemisphere surface climate. *Nature Climate Change*, *6*(10), 917–926. Retrieved from `http://dx.doi.org/10.1038/nclimate3103` doi: 10.1038/nclimate3103

Kay, J. E., Deser, C., Phillips, A., Mai, A., Hannay, C., Strand, G., ... Vertenstein, M. (2015). The community earth system model (CESM) large ensemble project : A community resource for studying climate change in the presence of internal climate variability. *Bulletin of the American Meteorological Society*, *96*(8), 1333–1349. doi: 10.1175/BAMS-D-13-00255.1

Kirchmeier-Young, M. C., Zwiers, F. W., & Gillett, N. P. (2017). Attribution of extreme events in Arctic Sea ice extent. *Journal of Climate*, *30*(2), 553–571. doi: 10.1175/JCLI-D-16-0412.1

Kuttippurath, J., & Nair, P. J. (2017). The signs of Antarctic ozone hole recovery. *Scientific Reports*, *7*(1), 1–8. Retrieved from `http://dx.doi.org/10.1038/`

s41598-017-00722-7 doi: 10.1038/s41598-017-00722-7

Landrum, L. L., Holland, M. M., Raphael, M. N., & Polvani, L. M. (2017). Stratospheric Ozone Depletion: An Unlikely Driver of the Regional Trends in Antarctic Sea Ice in Austral Fall in the Late Twentieth Century. *Geophysical Research Letters*, *44*(21), 11,062–11,070. doi: 10.1002/2017GL075618

Lenaerts, J. T., Fyke, J. G., & Medley, B. (2018). The signature of ozone depletion in recent Antarctic precipitation change: a study with the Community Earth System Model. *Geophys. Res. Lett.*, *45*, 12931—-12939. doi: 10.1029/2018GL078608

Lenaerts, J. T., Vizcaino, M., Fyke, J., van Kampenhout, L., & van den Broeke, M. R. (2016). Present-day and future Antarctic ice sheet climate and surface mass balance in the Community Earth System Model. *Climate Dynamics*, *47*(5-6), 1367–1381. doi: 10.1007/s00382-015-2907-4

Maher, N., Milinski, S., & Ludwig, R. (2021). Large ensemble climate model simulations: introduction, overview, and future prospects for utilising multiple types of large ensemble. *Earth System Dynamics*, *12*(2), 401–418. Retrieved from https://esd.copernicus.org/articles/12/401/2021/ doi: 10.5194/esd-12-401-2021

Marshall, G. J., & Thompson, D. W. (2016). The signatures of large-scale patterns of atmospheric variability in Antarctic surface temperatures. *Journal of Geophysical Research*, *121*(7), 3276–3289. doi: 10.1002/2015JD024665

Marshall, G. J., Thompson, D. W., & van den Broeke, M. R. (2017). The Signature of Southern Hemisphere Atmospheric Circulation Patterns in Antarctic Precipitation. *Geophysical Research Letters*, *44*(22), 11,580–11,589. doi: 10.1002/2017GL075998

Medley, B., & Thomas, E. R. (2019). Increased snowfall over the Antarctic Ice Sheet mitigated twentieth-century sea-level rise. *Nature Climate Change*, *9*(1), 34–39. Retrieved from http://dx.doi.org/10.1038/s41558-018-0356-x doi: 10.1038/s41558-018-0356-x

Nicolas, J. P., & Bromwich, D. H. (2014). New reconstruction of antarctic near-surface temperatures: Multidecadal trends and reliability of global reanalyses. *Journal of Climate*, *27*(21), 8070–8093. doi: 10.1175/JCLI-D-13-00733.1

O'Connor, G. K., Steig, E. J., & Hakim, G. J. (2021). Strengthening Southern

Hemisphere Westerlies and Amundsen Sea Low Deepening Over the 20th Century Revealed by Proxy-Data Assimilation. *Geophysical Research Letters*, *48*(24). doi: 10.1029/2021gl095999

Raphael, M. N., Marshall, G. J., Turner, J., Fogt, R. L., Schneider, D., Dixon, D. A., ... Hobbs, W. R. (2016). The Amundsen sea low: Variability, change, and impact on Antarctic climate. *Bulletin of the American Meteorological Society*, *97*(1), 111–121. doi: 10.1175/BAMS-D-14-00018.1

Ribes, A., & Terray, L. (2013). Application of regularised optimal fingerprinting to attribution. Part II: Application to global near-surface temperature. *Climate Dynamics*, *41*(11-12), 2837–2853. doi: 10.1007/s00382-013-1736-6

Smith, K. L., & Polvani, L. M. (2017). Spatial patterns of recent Antarctic surface temperature trends and the importance of natural variability: lessons from multiple reconstructions and the CMIP5 models. *Climate Dynamics*, *48*(7-8), 2653–2670. doi: 10.1007/s00382-016-3230-4

Steig, E. J., Schneider, D. P., Rutherford, S. D., Mann, M. E., Comiso, J. C., & Shindell, D. T. (2009). Warming of the Antarctic ice-sheet surface since the 1957 International Geophysical Year. *Nature*, *457*(7228), 459–462. doi: 10.1038/nature07669

Swart, N. C., Gille, S. T., Fyfe, J. C., & Gillett, N. P. (2018). Recent Southern Ocean warming and freshening driven by greenhouse gas emissions and ozone depletion. *Nature Geoscience*, *11*(11), 836–841. Retrieved from `http://dx.doi.org/10.1038/s41561-018-0226-1` doi: 10.1038/s41561-018-0226-1

Thomas, E. R., Hosking, J. S., Tuckwell, R. R., Warren, R. A., & Ludlow, E. C. (2015). Twentieth century increase in snowfall in coastal West Antarctica. *Geophysical Research Letters*, *42*(21), 9387–9393. doi: 10.1002/2015GL065750

Thompson, D. W. J., Solomon, S., Kushner, P. J., England, M. H., Grise, K. M., & Karoly, D. J. (2011). Signatures of the Antarctic ozone hole in Southern Hemisphere surface climate change. *Nature Geoscience*, *4*(11), 741–749. Retrieved from `http://www.nature.com/doifinder/10.1038/ngeo1296` doi: 10.1038/ngeo1296

Turner, J., Colwell, S. R., Marshall, G. J., Lachlan-Cope, T. A., Carleton, A. M., Jones, P. D., ... Iagovkina, S. (2004). The SCAR READER project: Toward

a high-quality database of mean Antarctic meteorological observations. *Journal of Climate*, *17*(14), 2890–2898. doi: 10.1175/1520-0442(2004)017⟨2890:TSRPTA⟩2.0.CO;2

Turner, J., Colwell, S. R., Marshall, G. J., Lachlan-Cope, T. A., Carleton, A. M., Jones, P. D., ... Iagovkina, S. (2005). Antarctic climate change during the last 50 years. *International Journal of Climatology*, *25*(3), 279-294. Retrieved from https://rmets.onlinelibrary.wiley.com/doi/abs/10.1002/joc.1130 doi: https://doi.org/10.1002/joc.1130

Turner, J., Comiso, J. C., Marshall, G. J., Lachlan-Cope, T. A., Bracegirdle, T., Maksym, T., ... Orr, A. (2009). Non-annular atmospheric circulation change induced by stratospheric ozone depletion and its role in the recent increase of Antarctic sea ice extent. *Geophysical Research Letters*, *36*(8), 1–5. doi: 10.1029/2009GL037524

Supporting References

Allen, M. R., & Stott, P. A. (2003). Estimating signal amplitudes in optimal fingerprinting, part I: Theory. *Climate Dynamics*, *21*(5-6), 477–491. doi: 10.1007/s00382-003-0313-9

Gillett, N. P., Kirchmeier-Young, M., Ribes, A., Shiogama, H., Hegerl, G. C., Knutti, R., ... Ziehn, T. (2021). Constraining human contributions to observed warming since the pre-industrial period. *Nature Climate Change*, *11*(3), 207–212. Retrieved from https://doi.org/10.1038/s41558-020-00965-9 doi: 10.1038/s41558-020-00965-9

Ribes, A., Planton, S., & Terray, L. (2013). Application of regularised optimal fingerprinting to attribution. Part I: Method, properties and idealised analysis. *Climate Dynamics*, *41*(11-12), 2817–2836. doi: 10.1007/s00382-013-1735-7

Tett, S. F., Stott, P. A., Allen, M. R., Ingram, W. J., & Mitchell, J. F. (1999). Causes of twentieth-century temperature change near the Earth's surface. *Nature*, *399*(6736), 569–572. doi: 10.1038/21164